



## Microstructure and optical properties of lustre glazes produced on a copper body

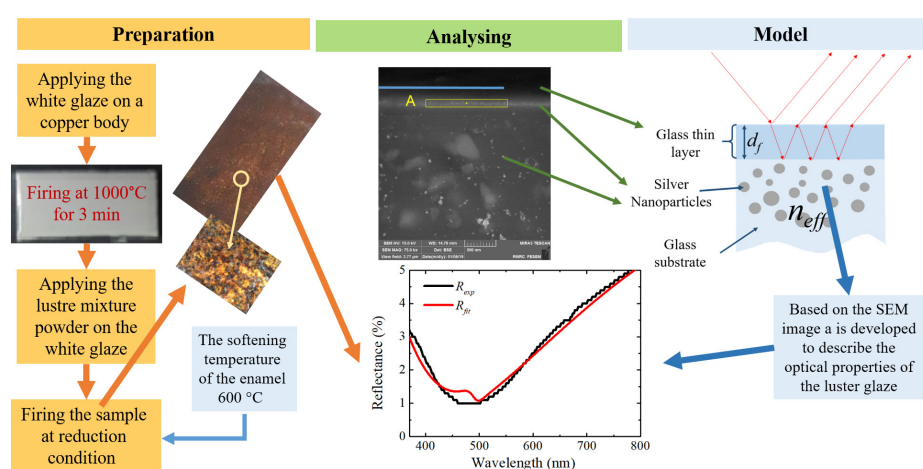
Tahereh Usefzaei, Majid Rashidi Huyeh<sup>✉</sup>, Reza Jabiri

Department of Physics, Faculty of Science, University of Sistan and Baluchestan, Zahedan, Iran

### HIGHLIGHTS

- Applying the suitable lustre substrate, on the copper body and finding optimal temperature for lustre firing.
- A suitable mixture powder is proposed and the optimal condition of firing were found.
- A theoretical model proposed to simulate the optical properties of the produced samples.

### GRAPHICAL ABSTRACT



### ARTICLE INFO

Article type:

Research article

Article history:

Received 29 January 2024

Received in revised form 24 February 2024

Accepted 28 February 2024

Keywords:

Lustre glaze

Enamel glaze

Noble metal nanoparticles

Thin film

Surface plasmon resonance

DOI: [10.22104/JPST.2024.6725.1249](https://doi.org/10.22104/JPST.2024.6725.1249)

### ABSTRACT

In this research, a lustre enamel is applied to a copper body. A white glaze, conventionally applied in enamel handcraft, was used as the lustre substrate. Silver nitrate was used as the source of the lustre metal. Since the work aimed to determine the optimal firing conditions, several samples were prepared with different reduction temperatures and times. The optimal firing temperature and reduction time were found to be 600 °C and 10 min, respectively. The microstructure and chemical analyses were performed on the samples using an FE-SEM image. The results showed the successful formation of silver nanoparticles within the glaze substrate. In addition, two layers were formed: a thin glass layer of several tens of nm on the surface and a layer containing silver nanoparticles inside the glaze. The results also showed that the silver nanoparticles can penetrate several microns into the glaze body. Reflectance spectra confirmed the presence of silver nanoparticles in the lustre with a volume fraction of order of 0.01%.



© The Author(s).

Published by IROST.

## 1. Introduction

For a long time, metal nanoparticles such as gold, silver, copper, and iron have been used by craftsmen and artists to color and decorate objects. For example, the presence of gold-silver alloy nanoparticles in the Lycurgus Cup (400 BC) causes a green/yellow color in reflection and a purple-red color in transmission [1]. Metal glazes have been created to add value and beauty to objects. Several methods have been developed for this purpose, among which luster glaze is very important [2,3].

To produce a luster glaze, compounds of silver and copper are first mixed with a mixture of metal salts and clay and applied to the glass body. Then, the coated object is heated to the softening temperature of the glass substrate in a reducing atmosphere, resulting in reduced silver and copper ions. These ions penetrate into the glass as a result of ion exchange with potassium and sodium ions. Finally, the silver and copper ions join inside the glass substrate and form silver and copper nanoparticles, forming a luster glaze due to the reaction between the luster and the glass substrate on the surface. The properties of the lustre enamel, such as the nature and size of nanoparticles, the position and thickness of the layer, and the distribution of particles in the layer, depend on the materials and the firing process [4-8]. The lustre glaze consists of a micrometer glass layer containing silver and/or copper nanoparticles located under a superficial glass layer. Various colors can be obtained by altering the concentration, type, and size of the particles as well as the thickness of the layers. Due to the simultaneous presence of silver and copper in their structure, the initial lustre glazes could form several colors; however, the next generation of the lustre glazes was monochromatic due to the absence of copper [9].

Specular reflection, which provides a quasi-metallic shine, is a crucial feature of lustre glaze. The difference between lustre glaze and other metal-containing glazes lies in the fact that in lustre glaze, nanoparticles penetrate several micrometers into the glaze. In 'raku ware', the metal is applied to the entire glaze. In another method, a resin containing metal nanoparticles is applied to the body. The resin is a low-temperature glass mixture that, after firing, forms a glass layer attached to the glaze surface like an enamel but contains metallic nanoparticles [2].

Ongoing developments in nanoscience and nanotechnology have resulted in a lot of research on lustre glazes. Some of this research has focused on their historical aspects, with many studies dealing with the luster glazes' structure, microstructure, and optical properties [10-16]. Some researchers have also tried to reproduce lustre glaze [16-21]. By using a systematic knowledge of the physics governing this phenomenon, modern science, and the experience of the predecessors, it

is possible to consider new applications for this technique. For the first time, this paper reports a method of applying lustre glaze on a copper metal body. The microstructural and optical characteristics of the produced lustre glaze have also been investigated and discussed. A primitive model, based on multi-beam interference, is presented to study the optical properties of the lustres.

## 2. Experimental

### 2.1. Materials

White enamel was produced by using commercial enamel powder. The materials used to prepare the luster glaze were silver nitrate, copper oxide, iron oxide, mercury sulfate, clay, and acetic acid. Table 1 lists the raw materials and their chemical formula. The constituents of the clay used in the preparation of the luster powder are listed in Table 2.

**Table 1.** Raw materials used in the preparation of luster glaze.

Material	Chemical formula	Purity	Company
Silver nitrate	AgNO <sub>3</sub>	≥ 99%	Merck
Copper oxide	CuO	≥ 99%	Merck
Iron(III) oxide	Fe <sub>2</sub> O <sub>3</sub>	≥ 99%	Merck
Mercury(II) sulfate	HgSO <sub>4</sub>	≥ 98.5 %	Merck
Acetic acid	CH <sub>3</sub> COOH	100%	Merck
Hydrochloric acid	HCl	32%	Ghatran Shimi
Nitric acid	HNO <sub>3</sub>	65%	Ghatran Shimi
Clay	(see Table 2)	-	-

**Table 2.** XRF element analysis of the clay used in the preparation of luster glaze.

Oxide	Chemical formula	Mole percent (%)
Silica	SiO <sub>2</sub>	55.484
Sodium oxide	Na <sub>2</sub> O	1.077
Calcium oxide	CaO	22.393
Magnesium oxide	MgO	7.618
Alumina	Al <sub>2</sub> O <sub>3</sub>	8.618
Iron (III) oxide	Fe <sub>2</sub> O <sub>3</sub>	2.462
Potassium oxide	K <sub>2</sub> O	1.769
Titanium oxide	TiO <sub>2</sub>	0.446
Trace and LOI		17.907

## 2.2. Preparation of copper body

Copper sheets with a purity of 99.9% were cut into  $2 \times 3$  cm<sup>2</sup> pieces. It is well-known that the adhesion of glazes to the metal surface depends on the cleanliness of the surface. Accordingly, the surface of the copper body was prepared in four stages, see Fig. 1. The samples were first degreased with a nitric acid solution for 10 min, followed by deoxidization by washing the samples with alcohol for 5-10 min. After that, the samples were washed with distilled water and, finally, dried in ambient conditions.

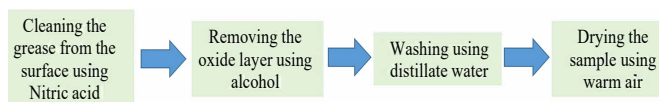


Fig. 1. Copper body preparation steps.

## 2.3. Preparation of white enamel

A slurry of enamel powder was first prepared to make the white enamel for use as a substrate for the luster glaze. These powders contain combinations of different oxides, a significant fraction of which is silica. Two methods were used to create enamel on the copper sheets: immersion and spraying. In the immersion method, copper sheets were immersed in enamel slurry and then dried at ambient temperature. These pieces were then fired at 900 °C for 10 min. Macro images of the samples prepared by this method are shown in Fig. 2(a). It can be seen that the glass layer is well formed on the copper sheet, but the surface is not uniform and smooth. The glaze is wavy, and its roughness is not desirable. Therefore, in the next step, the spraying method was used, and the firing temperature was increased to 1000 °C while the firing time was reduced to 3 min. Fig. 2(b) shows the images of the prepared samples. As can be seen, the glass layer is well-formed, and the sample's surface is smooth and uniform. It should also be noted that the enamel does not separate from the copper surface during cooling because of the difference in values between the thermal expansion of copper and the white enamel.

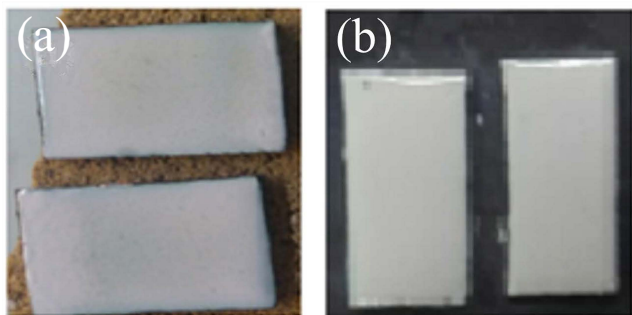


Fig. 2. Macro-images of the prepared white enamel applied on the copper bodies using (a) immersion and (b) spraying methods.

## 2.4. Preparation of luster glaze

Silver nitrate was used to introduce silver nanoparticles into the white enamel. Also, copper oxide was used as a reducing agent for silver ions. It can also be converted into copper metal ions under strong reduction conditions to form copper nanoparticles. Mercury-containing compounds were added as melting aids to lower the reaction temperature between the luster mixture and the white enamel. Iron oxide was added as a reducing agent, while clay was used as filler. Acetic acid was used as a homogenizer, and sawdust and graphite were used to create reduction conditions. The raw materials were weighed by a digital scale with an accuracy of 0.0001 to 0.01, depending on the material. Then, the lustre mixture was ground and softened in a laboratory mortar for half an hour. After the addition of acetic acid, this step was continued for another half an hour until a homogeneous and uniform mixture was obtained. It should be noted that grinding the materials and preparing the powder into fine grains improves the penetration of the materials and the formation of a uniform layer. Lastly, a thin layer of the mixture was applied on the surface of the previously cleaned white enamel with a fine brush.

After air drying, the samples were placed in an alumina crucible, as shown in Fig. 3. The crucible was then placed in a container filled with sawdust (or graphite) as a reducing agent. The crucible lid was completely sealed to prevent the entry of sawdust or carbon monoxide gas during the reduction process. Next, the container was also sealed tightly to prevent any exchange with the outside atmosphere and then placed in the oven. After cooling for about 24 h, the samples were removed from the oven, the ash on the surface of the samples was removed, and they were cleaned with ethanol and distilled water.

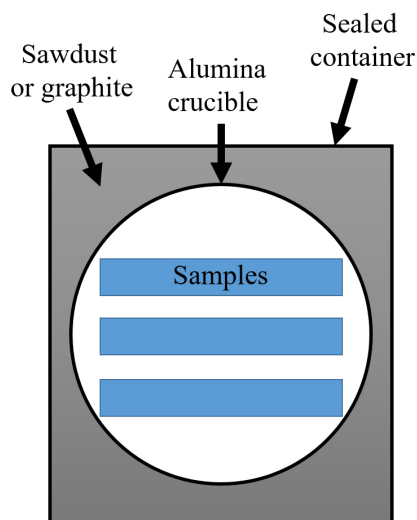


Fig. 3. Schematic representation of samples placed in an alumina crucible embedded by sawdust (or graphite) in a sealed container.

Five samples (M1 to M5) were prepared with the composition shown in Table 3 under different reducing conditions. These values were adopted according to the previous work [17,18]. The firing conditions, such as reduction temperature, reduction time, and the reducing agent for each sample, are given in Table 4. Graphite was used as a reducing agent for the M1 and M2 samples, while other samples were reduced in the presence of sawdust.

Optical microscopy images of the produced samples at low and high magnifications are shown in Fig. 4. As can be seen, the surface of the M1 sample is completely dull and black without a metallic luster. Therefore, the temperature was reduced from 600 to 550 °C for the M2 sample. Again, a nonuniform color distribution was observed on the surface, and the glaze surface was also black and matte. However, brown and green textures also appeared in addition to the dark textures. In the M3 sample, the reduction time was reduced from 15 to 10 min. As can be observed, the color is poor, and the sample did not show metallic lustre. Only faint lustre spots were observed, and the particles were spread unevenly on the glaze surface. In the case of the M4 sample, the temperature was increased to 570 °C, resulting in a smooth and transparent surface with uniform color with an attractive lustre. This slight color change and low colored zone can be attributed to the low firing temperature. In the M5 sample, the temperature was increased to 600 °C. As can be seen, the color of the glaze is light brown, which indicates the presence of copper in the lustre enamel. The surface also shows a unique metallic luster. This sample was considered the optimal sample for the subsequent analyses.

**Table 3.** Chemical composition of the lustre glaze.

Material	Chemical Formula	Weight percent (%)
Silver nitrate	AgNO <sub>3</sub>	4.80
Copper oxide	CuO	11.57
Mercury(II) sulfate	HgSO <sub>4</sub>	34.70
Iron(III) oxide	Fe <sub>2</sub> O <sub>3</sub>	4.50
Clay	(See Table 2)	44.43

**Table 3.** Reduction conditions applied to different samples.

Sample	M1	M2	M3	M4	M5
Reduction temperature (°C)	600	550	550	570	600
Reduction time (min)	15	15	10	10	10
Reducing agent	Graphite	Graphite	Sawdust	Sawdust	Sawdust

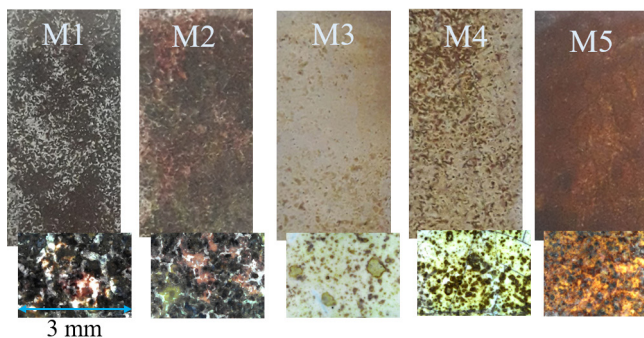


**Fig. 4.** Optical images of the samples at low (top) and high (bottom) magnifications.

### 2.5. Characterization

A field emission scanning electron microscope (FESEM, MIRA3TESCAN-XMU) equipped with EDX micro-analysis was used for structural investigation. A Dilatometer (Dama Pajohe Arvin, Horizontal Dil-101) was used to determine the softening temperature of the glaze. Also, the reflection spectrum of the samples was measured using a spectrophotometer (PG instrument Double Beam T80 series). X-ray fluorescence spectroscopy (XRF, Philips PW1410) was used for elemental analysis.

## 3. Results and discussion

### 3.1. White enamel

As mentioned, lustre glaze should be fired at the softening temperature of the glaze enamel [5]. This was determined using a dilatometer. Fig. 5 shows the relative length change of a white enamel cylindrical sample of about 1cm in length with temperature. The maximum value is at the temperature of 560 °C, which can be considered as the softening temperature of the enamel. This temperature indicates the firing temperature of the lustre and corresponds to the reported values [5].

Fig. 6 shows the FE-SEM image from the cross-section of the white enamel. The fine bright spots in this image are mainly made of titanium. This can be confirmed by the EDX elemental map of the lustre glaze shown in Fig. 7(b), which will be explained later. The chemical composition of the white enamel on the copper body was also determined

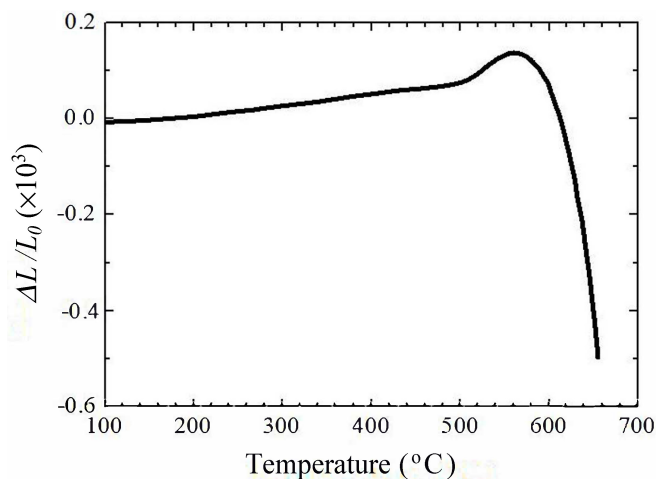


**Fig. 5.** Thermal analysis of white enamel showing its softening temperature.

using the EDX elemental analysis. Fig. 6 also shows the EDX analysis of the cross-section of the white enamel. The results obtained based on the mole percentage of the elements are shown in the inset of Fig. 6(b). The results show that the enamel mainly consists of silica and oxygen, the main glass-making elements.

3.2. Luster glaze

Fig. 7(a) shows the FE-SEM image from the cross-section of the M5 sample. The surface is roughly marked by a horizontal line. About 50 nm below the surface, a layer consisting of bright spots can be distinguished (rectangle A). Of course, other bright spots are somehow noticeable throughout the sample. The distribution of oxygen, silicon, aluminum, titanium, potassium, and silver elements can be seen in the EDX elemental map, shown in Fig. 7b. It can be seen that oxygen and aluminum are evenly distributed throughout the cross-section of the sample, while the situation is different

for titanium, silicon, potassium and, especially, silver. It is evident that the concentration of titanium increases from the surface to the depth of the sample, reaching its highest levels in the areas where bright spots are present. Therefore, these microparticles are mainly made of titanium (titanium oxide), which is present in the white enamel. While the concentration of potassium and silicon decreased near the surface, the concentration of silver increased near the surface of the sample. This behavior is attributed to the ion exchange between the glass substrate and luster powder. During heating, the potassium ions in the glass substrate are replaced by the silver ions reduced in the luster glaze [9,16]. Therefore, the bright spots near the surface that were observed in the FE-SEM image represent silver nanoparticles. In the combined silver-silica elemental map, the concentration of silver on the surface of the sample is higher than that at greater depths.

Fig. 8 and its inset show the EDX elemental analysis of the surface of the M5 sample (rectangle A in Fig. 7(a)). The comparison of the concentrations of aluminum, silicon, and oxygen in white enamel (inset of Fig. 6(b)) with those in luster glaze reveals that the oxygen and aluminum concentrations in the luster glaze have increased compared to the white enamel, while silicon has decreased. This can indicate the penetration of aluminum from the luster powder into the glass substrate during firing. As a result, the prepared luster glaze is composed of a glass layer with a thickness of several tens of nanometers and a micrometer layer enriched with silver nanoparticles on a glass substrate. This microstructure was also reported by other researchers [15,22].

3.3. Optical properties

To study the optical properties of the produced samples, the reflection spectra of the white enamel as well as M3, M4, and M5 samples were recorded, as shown in Fig. 9. As can be

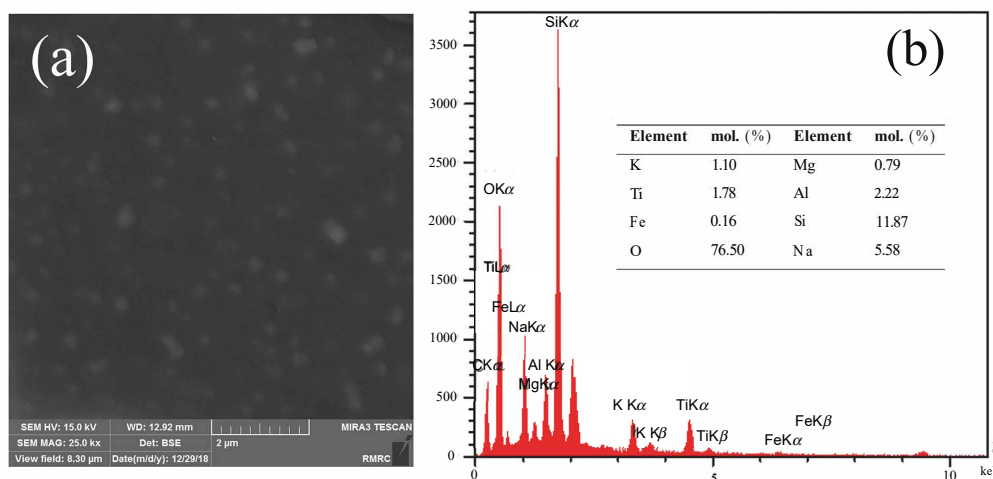


**Fig. 6.** (a) FE-SEM image from a cross-section of the white enamel on the copper body, and (b) EDX analysis of the white enamel, the inset represents the percentage of chemical composition values.

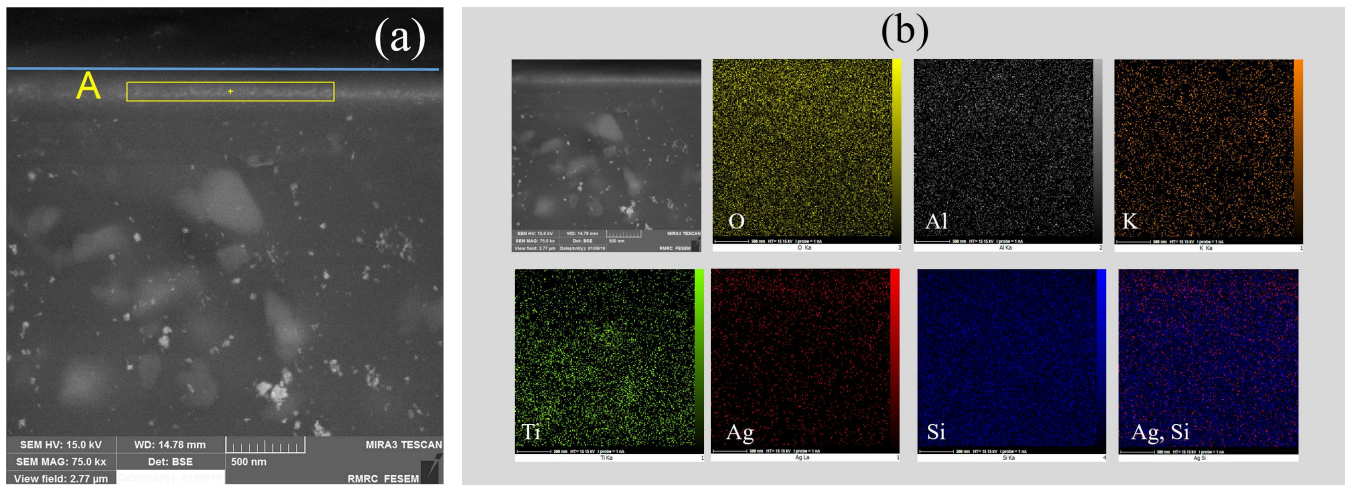


**Fig. 7.** (a) FE-SEM image from a cross-section of M5 sample. Rectangle A represents the layer enriched with silver nanoparticles near the surface. (b) FE-SEM images from the cross-section show (O) the EDX elemental map of oxygen (O), (Al) aluminum, (K) potassium, (Ti) titanium, (Ag) silver, (Si) silicon, and (Ag-Si) combined silver-silicon maps.

seen, the reflection spectrum of white enamel (black curve) shows a constant value in all wavelengths. Also, there is no significant change in the reflection spectrum of the M3 sample (red curve), which has a low color concentration. However, the reflection spectrum of the M4 and M5 samples varies significantly. This behavior is mainly due to the presence of a thin glass layer on the surface as well as a layer containing silver nanoparticles on the glass substrate. The change in the color of the glaze in different places is due to changes in the lustre glaze's thickness and microstructure, especially the concentration and size of the silver nanoparticles in different parts of the lustre glaze. The minimum values observed in the reflection spectra of the M4 and M5 samples are due to the absorption of light by silver nanoparticles, which are linked to the surface plasmon resonance. This phenomenon is due to the harmonic oscillations of the free electrons of silver nanoparticles, which leads to light absorption at a frequency known as the surface plasmon resonance frequency [23]. This

frequency is dependent on the shape and dimension of the nanoparticles as well as their host medium. In the following, a model based on multi-beam interference is presented to investigate the optical properties of the lustre glaze.

### 3.4. Modelling

In this section, a model will be presented to describe the optical properties of the lustre glaze. As mentioned earlier, the lustre microstructure consists of a thin glass layer on a layer of silver nanoparticles embedded in a glass substrate (Fig. 10). Therefore, the reflection spectrum is mainly caused by the interference of reflection waves from the air-glass interface and the glass-layer containing silver nanoparticles. In this way, the reflection spectrum of the samples can be obtained according to the interference of reflection waves from the lustre glaze in the form of Eq. (1).

$$R = |r^2| \tag{1}$$

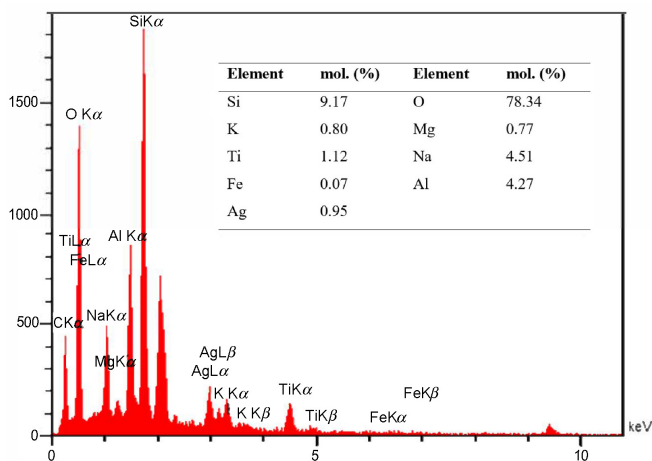


**Fig. 8.** EDX analysis of rectangle A shown in Fig. 7(a); the inset represents the chemical composition values.

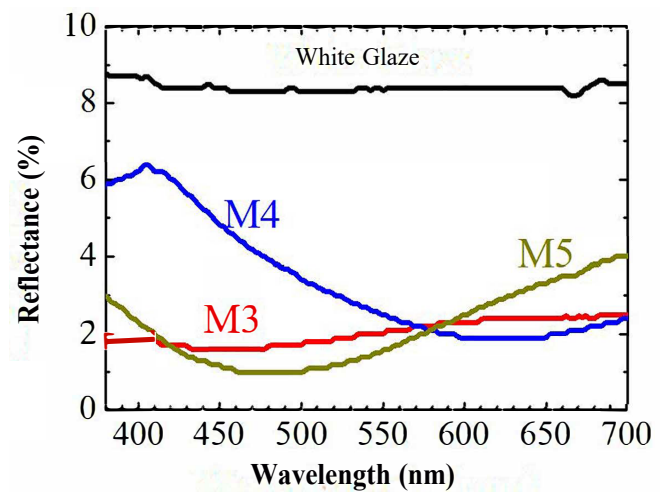


**Fig. 9.** Reflectance spectra of white enamel and lustre glazes (M3, M4, and M5).

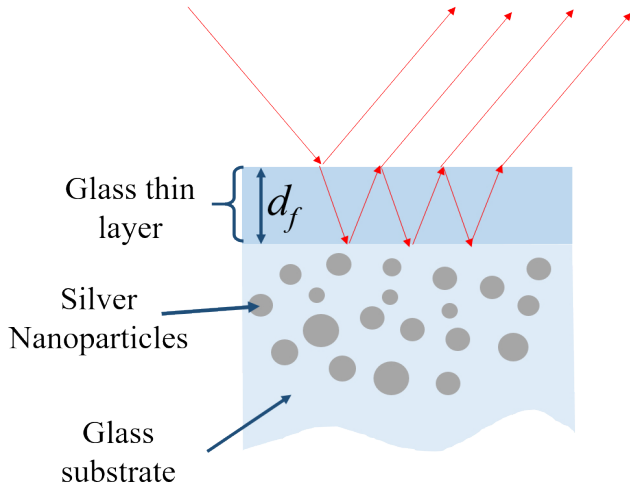


**Fig. 10.** Proposed diagram of the luster microstructure consists of a thin glass layer on a layer of silver nanoparticles embedded in a glass substrate.

where  $r$  is the reflection amplitude of the sample, which is obtained based on the interference of the reflected beams from the thin glass layer according to the following equation [22,24]:

$$r = \frac{r_0 + r_1 e^{2i\beta}}{1 + r_0 r_1 e^{2i\beta}} \quad (2)$$

where  $\beta = \frac{2\pi}{\lambda} n_j d_f$  is the phase difference of two successive reflected beams from lustre glaze interfaces, and  $d_f$  and  $n_j$  are the thickness and refractive index of the thin glass layer, respectively.  $r_0$  and  $r_1$  are the Fresnel reflection coefficients from the air-thin layer and thin layer-glass substrate interfaces. The reflection coefficients of  $r_{ij}$  from an interface of  $i$  and  $j$  media for s (parallel) and p (perpendicular) polarizations according to the Fresnel equations are:

$$(r_{ij})_s = \frac{n_i \cos(\theta_i) - n_j \cos(\theta_j)}{n_i \cos(\theta_i) + n_j \cos(\theta_j)} \quad (3)$$

$$(r_{ij})_p = \frac{n_j \cos(\theta_i) - n_i \cos(\theta_j)}{n_j \cos(\theta_i) + n_i \cos(\theta_j)}$$

where  $n_i$  and  $n_j$  are the refractive indices of  $i$ th and  $j$ th medium, respectively.  $\theta_i$  and  $\theta_j$  are the incident and refractive angles, respectively. The refractive index of silver nanoparticles embedded in the glass substrate ( $\tilde{n}_{eff}$ ) can be expressed by the Maxwell-Garnett effective medium theory [25].

$$\tilde{n}_{eff} = \sqrt{\tilde{\epsilon}_{eff}} = \sqrt{\epsilon_g \frac{\tilde{\epsilon}_{Ag}(1+2p) + 2\epsilon_g(1-p)}{\tilde{\epsilon}_{Ag}(1-p) + \epsilon_g(2+p)}} \quad (4)$$

where  $\tilde{\epsilon}_{Ag}$  is the dielectric function of silver,  $\epsilon_g$  is the dielectric function of the nanoparticle host medium, and  $p$  is the volume fraction of silver nanoparticles.

The reflectance of the white enamel according to the Fresnel equations in a normal incident is:

$$R_0 = \left| \frac{1 - n_s}{1 + n_s} \right|^2 \quad (5)$$

where  $n_s$  is the refractive index of the white enamel.

According to the reflectance spectrum of the white enamel (black curve in Fig. 9), the value of  $R_0$  is a constant value of 8.6%. Therefore, the refractive index of white enamel, calculated using Eq (5), is 1.73. It is necessary to explain that the roughness of the surface may cause some errors in the measurement of  $R_0$  and hence  $n_s$  values. Then, the measured reflectance spectra of the lustres were fitted using Eq. (1). In this fitting,  $d_f$ ,  $n_j$ ,  $p$ , and  $n_g$  were considered as free parameters. Fig. 11 shows the results of fitting the reflectance spectrum of the M5 sample. As can be seen, there is a very good agreement between the fitting data and the experimental results. In particular, a minimum is observed at the wavelength of about 480 nm, which corresponds to the absorption increasing at the surface plasmon resonance wavelength. Table 5 shows the parameters obtained from the fitting data for M3, M4, and M5 samples. As can be seen, the volume fraction of silver in all the samples is in the range of 0.01%, which is in agreement with the reported values [7,8,22].

**Table 5.** The values obtained from fitting the reflectance spectra.

Parameter	Symbol	M3	M4	M5
Volume fraction of silver nanoparticles (%)	$p$	0.01	0.02	0.01
Thickness of the thin glass layer (nm)	$d_f$	98.23	98.23	37.32
Refraction index of the thin glass layer	$n_j$	1.57	1.57	1.52
Refractive index of the nanoparticle host medium	$n_g$	1.82	1.82	1.65

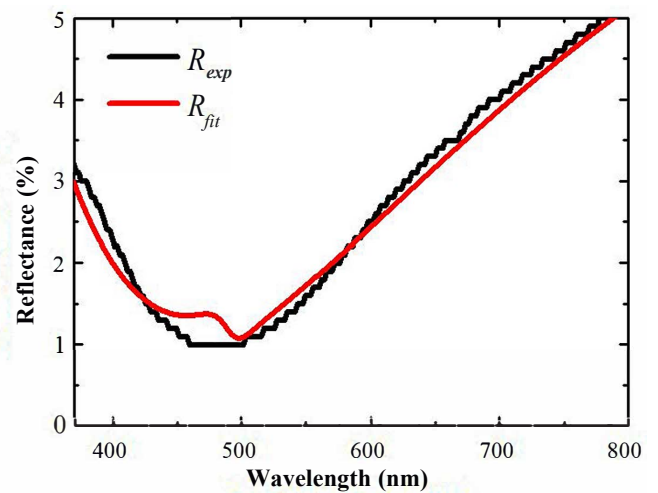


**Fig. 11.** Measured reflectance spectrum (black curve) and the modeled curve (red curve) for the M5 sample.

#### 4. Conclusion

Luster glazes were created on copper sheets for the first time. White enamel, conventionally applied in the enamel handcraft, was applied as a luster substrate. As the white enamel softening temperature is 560 °C, the lustre firing was done between 550 and 600 °C. The composition of the white enamel plays an important role during glazing and after firing. The optimal firing temperature was 600 °C with a redacting time of 10 min. FE-SEM images of the samples show the formation of luster glaze, including a thin glass layer on the surface and a layer containing silver nanoparticles embedded in the glass substrate. The reflectance of the lustre and hence its color is due to the presence of the silver nanoparticles and a thin glass layer on the surface of the lustre. A primitive model based on multi-beam interference was used to simulate the lustre reflectance. The simulation results showed an excellent agreement with the experimental ones. In particular, the volume fraction of silver was estimated to be in the order of 0.01%, corresponding to the values reported in the literature.

#### Acknowledgments

The authors would like to thank Mr. Amir Reza Gardeshzadeh for his scientific comments.

#### Disclosure statement

No potential conflict of interest was reported by the authors.

#### References

- [1] Barber, D. J., & Freestone, I. C. (1990). An Investigation of the Origin of the Colour of the Lycurgus Cup by Analytical Transmission Electron Microscopy. *Archaeometry*, 32, 33-45. <https://doi.org/10.1111/j.1475-4754.1990.tb01079.x>
- [2] Pradell T. (2016). Lustre and Nanostructures - Ancient Technologies Revisited. In Ph. Dillmann, L. Bellot-Gurlet, & I. Nenner (Eds.), *Nanoscience and Cultural Heritage* (pp. 3-39). Atlantis Press, The Netherlands. <https://doi.org/10.2991/978-94-6239-198-7>
- [3] Caiger-Smith, A. (1985). *Lustre Pottery: Technique, Tradition, and Innovation in Islam and the Western*, Faber and Faber.
- [4] Molina, G., Tite, M. S., Molera, J., Climent-Font, A., & Pradell, T. (2014). Technology of Production of Polychrome Lustre. *Journal of the European Ceramic Society*, 34, 2563-2574. <https://doi.org/10.1016/j.jeurceramsoc.2014.03.010>
- [5] Pradell, T., Molera, J., Bayés, C., & Roura, P. (2006). Luster Decoration of Ceramics: Mechanisms of Metallic Luster Formation. *Applied Physics A*, 83, 203-208. <https://doi.org/10.1007/s00339-006-3508-1>
- [6] Chabanne, D., Bouquillon, A., Aucouturier, M., Dectot, X., & Padeletti, G. (2008). Physico-Chemical Analyses of Hispano-Moresque Lustred Ceramic: A Precursor for Italian Majolica? *Applied Physics A*, 92, 11-18. <https://doi.org/10.1007/s00339-008-4458-6>
- [7] Molina, G., Murcia, S., Molera, J., Roldan, C., Crespo, D., & Pradell T. (2013). Color and Dichroism of Silver-Stained Glasses. *Journal of Nanoparticle Research*, 15, 1932. <https://doi.org/10.1007/s11051-013-1932-7>
- [8] Nikbakht, T., Kakuee, O., Montazerzohouri, M., Lamehi-Rachti, M., & Torkiha, M. (2019). Ionoluminescence Investigation of Medieval Iranian Luster Glazed Ceramics. *Journal of Luminescence*, 215, 116592. <https://doi.org/10.1016/j.jlumin.2019.116592>
- [9] Pradell, T., Molera, J., Smith, A. D., Climent-Font, A., & Tite, M. S. (2008). Technology of Islamic Lustre. *Journal of Cultural Heritage*, 9, e123-e128. <https://doi.org/10.1016/j.culher.2008.06.010>
- [10] Shams, A. H., Al-Karadawi, A. S., Eloriby, R. A. (2022). Chemical Characterization and Manufacturing Technology of Some Lustre Ceramic Dishes of the Abbasid Period, Northern Egypt. *Mediterranean Archaeology and Archaeometry*, 22(2), 50-66. <https://doi.org/10.5281/zenodo.6576803>
- [11] Pradell, T., Molera, J., Smith, A. D., & Tite, M. S. (2008). The Invention of Lustre: Iraq 9th and 10th Centuries AD. *Journal of Archaeological Science*, 35(5), 1201-1215. <https://doi.org/10.1016/j.jas.2007.08.016>
- [12] Montazer Zohouri, M., Torkiha, M., & Hesam, T. (2020). An Archaeological Study on the Provenance and Production of the Lusterware from the Underground Complex of Tappeh Ghaleh, Khomein, Iran Using PIXE. *Journal of Archaeological Studies*, 12(2), 205-224. <https://doi.org/10.22059/jarcs.2020.288850.142778>
- [13] Pradell, T., Molera, J., Smith, A. D., & Tite, M. S. (2008). Early Islamic lustre from Egypt, Syria and Iran (10th to 13th century AD). *Journal of Archaeological Science*, 35, 2649-2662. <https://doi.org/10.1016/j.jas.2008.05.011>
- [14] Mason, R. B. J. (2004). Shine like the sun: Lustre-Painted and Associated Pottery from the Medieval Middle East, Royal Ontario Museum.
- [15] Glòria Molina, G. (2014). *Colour and Technology in Historic Decorated Glazes and Glasses* [PhD Thesis], [Barcelona], Universitat Politècnica de Catalunya.
- [16] Pradell, T., Molera, J., Pantos, E., Smith, A. D., Martin C. M. & Labrador A. (2008). Temperature Resolved Reproduction of Medieval Luster. *Applied Physics A*, 90, 81-88. <https://doi.org/10.1007/s00339-007-4226-z>

- [17] Razavi, F., Ghahari, M., & Rashidi-Huyeh, M. (2014). Production and Characterization of a Lustre Glaze on Arcopal Body. *Journal of Technology and Science Color*, 8(1), 75-83. <https://dorl.net/dor/20.1001.1.17358779.1393.8.1.7.3>
- [18] Razavi, F., Rashidi Huyeh, M., & Ghahari, M. (2016). Production of Lustre Glaze on Opal Tableware Using Zarinfam Technique and Characterization of Its Structure and Color. *Applied Physics A*, 122, 490. <https://doi.org/10.1007/s00339-016-0012-0>
- [19] Gil, C., Villegas, M. A., & Fernandez Navarro, J. M. (2005). Preparation and Study of Superficially Coloured Lead Glass. *Journal of Materials Science*, 40, 6201-6206. <https://doi.org/10.1007/s10853-005-3155-5>
- [20] Mirshafiei, M., & Mohammadzadeh, M. (2015). Persian Lustre Glaze Making Based on Javaher Name-ye-Nezami. *Journal of Fine Arte: Visual*, 20(1), 59-66. <https://doi.org/10.22059/JFAVA.2015.55445>
- [21] Mohammadzadeh Mianji, M., & Ghassai, H. (2011). Preparation of Zarrin Faam Glaze (Luster Glaze) and Study of Effective Factors on Creation of Enamel Layer with Emphasize on Influence of Temperature and Thickness. *Journal of Technology and Science Color*; 5, 35-42. <https://dorl.net/dor/20.1001.1.17358779.1390.5.1.5.0>
- [22] Reillon, V., & Berthier, S. (2006). Modelization of the Optical and Colorimetric Properties of Lustrated Ceramics. *Applied Physics A*, 83, 257-265. <https://doi.org/10.1007/s00339-006-3492-5>
- [23] Khajegi P., & Rashidi-Huyeh M. (2021). Optical Properties of Gold Nanoparticles: Shape and Size Effects. *International Journal of Optics and Photonics (IJOP)*, 15(1), 41-48. <https://doi.org/10.52547/ijop.15.1.41>
- [24] Born, M., & Wolf, E. (1999). *Principles of Optics: Electromagnetic Theory of Propagation, Interference and Diffraction of Light* (7<sup>th</sup> ed.), Cambridge University Press.
- [25] Kreibig U., & Vollmer M. (1995). *Optical Properties of Metal Clusters*, Springer. <https://doi.org/10.1007/978-3-662-09109-8>

#### Additional information

Correspondence and requests for materials should be addressed to M. Rashidi Huyeh.

#### HOW TO CITE THIS ARTICLE

Usefzaei, T.; Rashidi Huyeh, M.; Jabiri, R. (2023). Microstructure and optical properties of lustre glazes produced on a copper body. *J. Part. Sci. Technol.* 9(2) 115-123.

DOI: [10.22104/JPST.2024.6725.1249](https://doi.org/10.22104/JPST.2024.6725.1249)

URL: [https://jpst.irost.ir/article\\_1370.html](https://jpst.irost.ir/article_1370.html)